

Effect of vehicle groups on heterogeneous disordered traffic flow

Akihito Nagahama¹, Nichika Asai¹, Claudio Feliciani², Xiaolu Jia³, and Katsuhiro Nishinari^{2,4}

- ¹ Graduate School of Informatics and Engineering, The University of Electro-Communications, 1-5-1 Chofugaoka, Chofu, Tokyo 182-8585, Japan, naga0862@uec.ac.jp
- ² Department of Aeronautics and Astronautics, School of Engineering, The University of Tokyo, 7-3-1 Hongo, Bunkyo-ku, Tokyo 113-8656, Japan
- ³ Beijing Key Laboratory of Traffic Engineering, Beijing University of Technology, 100 Pingleyuan, Chaoyang-district, 100124, Beijing, China
- ⁴ Research Center for Advanced Science and Technology, The University of Tokyo, 4-6-1 Komaba, Meguro-ku, Tokyo 153-8904, Japan

Abstract. In heterogeneous disordered traffic, where various vehicle types operate without strict lane discipline, self-organized vehicle groups often emerge. While the formation of such groups has been recognized, their influence on macroscopic traffic dynamics remains unclear. This study investigates how the prevalence and composition of vehicle groups affect flow–density relationships in heterogeneous disordered traffic. Using trajectory data from real-world video observations, we apply three distinct Passenger Car Unit (PCU) estimation methods to construct flow–density diagrams that account for traffic heterogeneity. The analysis reveals that group proportions, i.e., the proportion of vehicles that are classified as belonging to groups, have a nonlinear and traffic-situation-dependent impact on flow characteristics. Specifically, moderate group proportions (30–60%) are associated with higher flow rates in medium- and high-density conditions, whereas proportions exceeding 50% correspond to skewed traffic distributions toward low- or high-density extremes. Comparisons between vehicle-count-based and PCU-based group proportions indicate that normalization methods significantly affect the interpretation of group dynamics, particularly when groups consist mainly of small-PCU vehicles such as motorcycles. Additionally, lower group proportions enhance flow under free-flow conditions, while the entropy-based analysis indicates that the association between entropy alone and speed is not consistently observed across traffic situations. By contrasting representative trends and extreme high-flow cases, the results further suggest that traffic under similar density and group-proportion conditions can exhibit low-efficiency and high-efficiency modes. Overall, the findings highlight the importance of group prevalence in shaping macroscopic traffic dynamics, while suggesting that linking internal group composition to traffic performance may require richer structural descriptors beyond a single entropy measure. They offer valuable insights for developing bottom-up traffic control strategies tailored to heterogeneous traffic environments with limited infrastructure.

Keywords: Heterogeneous disordered traffic, mixed traffic, self-organized groups, group proportion, fundamental diagram

1 Introduction

The rapid proliferation of automobiles has played a crucial role in driving global economic growth in the 20th century, enhancing daily convenience, and facilitating the movement of people and goods. However, rapid population growth and economic development worldwide have led to increased motorization, exacerbating traffic congestion. Traffic congestion negatively impacts various aspects of society, including the economy, the environment, and public health. For instance, a study [5] estimated that in 2016, the European Union (EU) suffered an economic loss of approximately €200 billion, equivalent to 1.4% of its GDP, due to congestion. Traffic congestion is not solely a concern for developed countries. In developing countries, traffic congestion causes severe delays in urban mobility. According to a study [2], cities like Dhaka, Lagos, and Manila rank among the slowest in the world, with average travel times up to three times longer than those in the fastest cities. In Dhaka, for instance, average vehicular speed is less than one-third that of Flint, USA, resulting in substantial time losses for daily commuters and freight movement alike. Many other examples were also reported in literature [11, 27, 12]. In many developing regions, congestion is further exacerbated by the presence of diverse vehicle types, including motorcycles, three-wheelers, cars, and other various types of vehicles which often operate with minimal adherence to lane discipline. Such traffic conditions, characterized by a high degree of heterogeneity and disorder, are referred to in this study as heterogeneous disordered traffic.

In heterogeneous disordered traffic, various vehicle types exhibit self-organization behavior, which has been reported in several studies. For example, non-motorized vehicles such as bullock carts and bicycles, which move at significantly lower speeds, act as "moving obstacles." As a result, following vehicles tend to accumulate behind them, forming a long queue until they find an opportunity to overtake. This phenomenon leads to the formation of traffic platoons, as observed in previous research [26]. Apart from platoon formation, another widely studied form of self-organization in mixed traffic is the collective behavior of motorcycles. Lee [16] observed that motorcycles in mixed traffic conditions can demonstrate herd behavior, cycling through phases of filtering, gathering, and dispersing. This tendency enables motorcycles to self-organize dynamically within the traffic flow. Furthermore, Lee et al. [15] successfully replicated motorcycle queuing patterns at intersections using an agent-based model. Additionally, Das et al. [10] demonstrated that motorcycles create dynamic virtual lanes and engage in filtering behavior, further contributing to their self-organization.

An understanding and evaluation of the macroscopic characteristics and dynamics of 2D mixed traffic requires an analysis of the grouping behavior of different vehicles, including vehicle types other than motorcycles. Few studies have focused on groups of vehicles other than motorcycles. We previously suggested that different vehicle types (apart from motorcycles) tend to exhibit grouping behavior [23]. Furthermore, we have successfully detected specific groups in Indian traffic, where traffic flow is relatively smooth [24]. To identify groups, i.e., patterns of leader–follower relations, we introduced a new concept called frequent subnetworks in standardized traffic [24], which is referred to as "group" in the present study.

It has been suggested that in unmanaged and highly disordered traffic conditions, overall traffic capacity tends to decrease [4]. However, other studies have indicated that

the self-organization of vehicle formations in heterogeneous disordered traffic may contribute to improved traffic flow. Specifically, the spatial distribution and leader-follower relationships of particular vehicle types can influence overall traffic characteristics. Previous studies have demonstrated that, at least in lane-based heterogeneous traffic, the composition and sequence of vehicle types within a traffic platoon—where vehicles follow one another in a leader-follower relations—affect traffic stability and the emergence of stop-and-go waves [18, 8, 19]. These findings suggest that, in addition to the differences in driving behavior among vehicle types investigated in prior research [28, 1, 29, 21, 25], the specific combinations of vehicle types engaged in leader-follower interactions can also influence macroscopic traffic characteristics, in lane-based heterogeneous traffic. Furthermore, recent studies [17, 9] have attempted to quantitatively assess the extent to which different vehicle types exhibit cooperative behavior. This growing body of research highlights the increasing attention toward the relationship between inter-vehicle self-organization and traffic flow improvements in heterogeneous traffic.

Our previous studies [23, 24] quantitatively identified such spatially non-uniform self-organized vehicle formations, referred to as groups, in no-lane-based heterogeneous traffic. However, the impact of these groups on the traffic characteristics of heterogeneous disordered traffic remains unclear. The objective of this study is to determine whether the prevalence of groups influences the macroscopic traffic characteristics of heterogeneous disordered traffic, and if so, to elucidate the nature of this influence. To achieve this, we utilize several types of passenger car unit (PCU) to evaluate the fundamental diagram, enabling the evaluation of traffic characteristics while minimizing the influence of heterogeneity.

If this study successfully clarifies the influence of groups on the traffic flow of heterogeneous disordered traffic, it would suggest that self-organization driven by pragmatic driving [13] and mutual adjustments among drivers—as seen at unsignalized intersections [14], where drivers engage in implicit coordination and mutual adaptation—could also contribute to traffic flow improvements on roads where stop-and-go waves can occur. This finding has several significant implications for the field of traffic engineering. First, it reinforces the necessity of accurately reproducing spatially non-uniform vehicle distributions and self-organization in microscopic simulations of heterogeneous disordered traffic [22]. Additionally, by leveraging changes in traffic characteristics due to spatial clustering, in combination with lane or stop position separation [31] and driving support technologies enabled by Intelligent Transportation Systems (ITS), it may become feasible to achieve bottom-up traffic flow improvement even under minimal traffic regulations and predominantly pragmatic driving behaviors. More broadly, understanding how such decentralized, self-organizing traffic systems can improve efficiency through local interactions may offer insights into alternative models of societal governance, e.g., public space utilization, mobility, energy use, etc. Rather than relying solely on top-down, rule-based control, these findings support a paradigm in which local, autonomous behavior leads to emergent global benefits—a concept relevant not only to transportation but also to the broader design of resilient, adaptive social systems.

The remainder of this paper is structured as follows. Section 2 provides an overview of the video observation method, the extraction of vehicle trajectories, the classification of traffic situations, the technique for detecting vehicle groups, and the introduction of

PCU definitions used in this study. Section 3 investigates both general trends across group proportions and local variations within each group proportion using two complementary approaches: a smoothed analysis based on segment-wise medians and a detailed scatter plot visualization. We also examine whether the degree of vehicle-type mixing within a group is related to the flow performance in this section. Each subsection in this part includes both results and discussion. Section 4 provides discussion through the all results in Section 3. Finally, Section 5 presents the concluding remarks.

2 Data and Preprocessing

2.1 Observed Data and Vehicle Trajectory

The present study utilizes the same dataset employed in our prior work [24], which was collected through traffic observation conducted in Mumbai, India, over a four-day period from January 18 to 21, 2017. For detailed analysis, we selected a segment of video footage recorded on January 19 between 11:34 AM and 2:34 PM. The recording was made with a Sony HDR-CX670 video camera mounted on the second-floor balcony of a shopping mall.

Figure 1 presents a configuration of the observed road. The road section analyzed spans 35 meters in length and is enclosed by a red dashed rectangle. The location of the downstream traffic signal is indicated by a black chained rectangle just beyond the observation area.

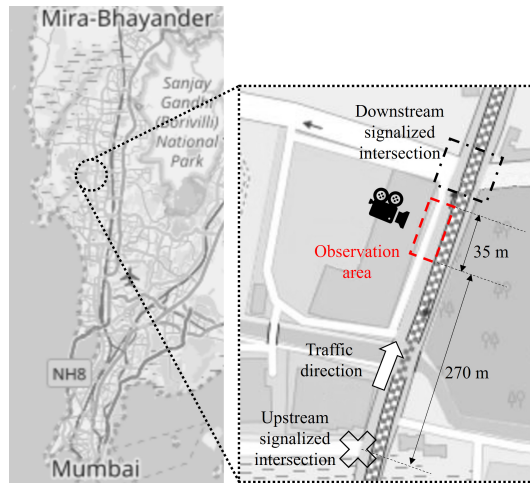


Fig. 1. Traffic-observation site used for data acquisition. The downstream signal, upstream intersection, and observation section are highlighted using a black chained rectangle, black cross mark, and red dashed rectangle, respectively. The map image is based on OpenStreetMap.

Vehicle positions in the image coordinate system were tracked semi-automatically using the Multiple Instance Learning (MIL) tracker from OpenCV [3]. Vehicle types

were manually classified into four categories: motorcycles (“m”), auto-rickshaws (three-wheelers, “r”), passenger cars (“c”), and heavy vehicles (“h”).

2.2 Classification of Traffic Situations

In the present study, we analyze a wide range of traffic situations, classified as follows:

- **All-flow (AF):** All traffic in the observation segment is steadily flowing.
- **Downstream-jammed (DJ):** Traffic is congested in the downstream area but remains flowing upstream.
- **All-jammed (AJ):** Traffic is congested throughout the entire observed segment.
- **Other (OT):** Traffic does not fall under the above categories (e.g., flow is beginning to recover downstream).

To classify the traffic situations, we utilized densities of several road segments. As illustrated in Fig. 2, the observation segment was divided into three zones: A, B, and C. These zones were delineated based on the positions of trees adjacent to the road. Traffic conditions within each zone were evaluated by calculating vehicle density, denoted as ρ_A , ρ_B , and ρ_C for Zones A, B, and C, respectively. Densities were computed for each video frame using the number of vehicles and the length of each zone.

Traffic situations were classified according to the following logic:

- **AF:** All densities are at or below the threshold $\rho_{th} = 0.6$ vehicles/m.
- **DJ:** Downstream densities exceed the threshold, while upstream densities are at or below the threshold.
- **AJ:** All densities exceed the threshold.
- **OT:** Conditions that do not meet any of the above definitions.

For example, a situation is classified as DJ when $\rho_A > \rho_{th}$, $\rho_B \leq \rho_{th}$, and $\rho_C \leq \rho_{th}$. Conceptually, AF corresponds to completely free-flowing traffic. DJ reflects partial congestion, primarily in downstream areas. AJ represents full congestion across the observed section, while OT is the situation wherein vehicles downstream begin to move freely while others are still in congestion.

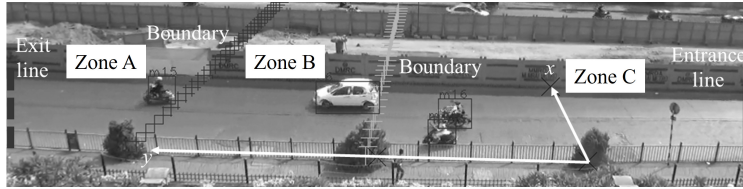


Fig. 2. Division of the observation segment into three zones (A, B, and C), arranged from downstream to upstream.

2.3 Detection of Groups

To distinguish between groups, we extracted groups from traffic data following the methodology established in our previous work [24]. While the full procedure is described in detail in that study, we provide a concise overview here. Figure 3 presents a flowchart summarizing the group detection process.

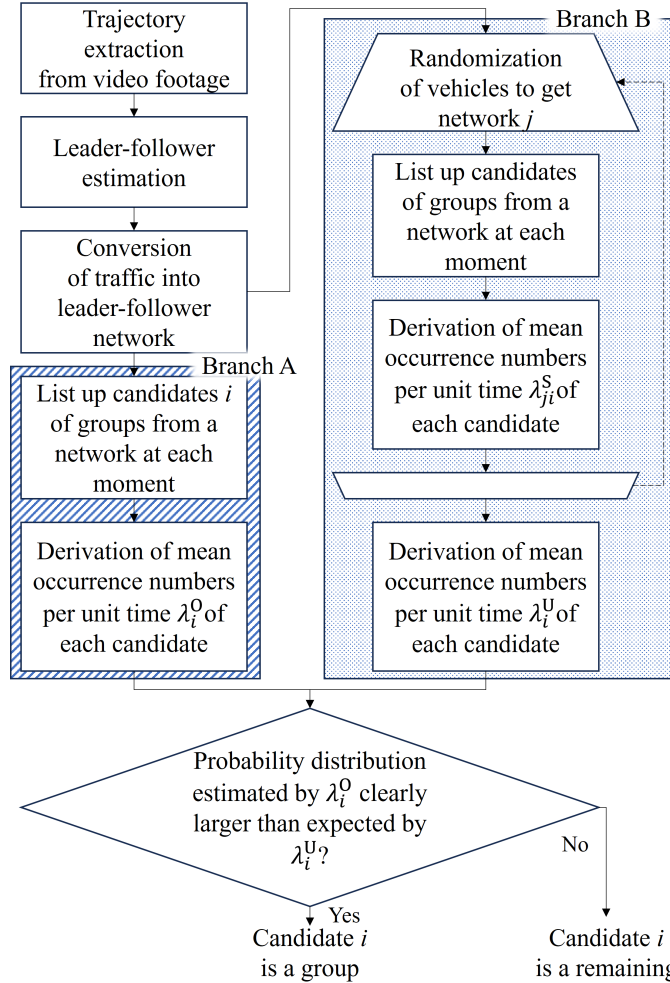


Fig. 3. Flowchart for classifying vehicles into groups and others.

The procedure begins by estimating each vehicle's trajectory from the video data and identifying leader-follower relationships—defined as instances where the acceleration or deceleration of a leading vehicle influences that of a following vehicle. In both the

current and prior studies, this relationship is determined based on two criteria: lateral proximity within a predefined threshold and adjacency of Voronoi cells.

By representing vehicles as nodes and their leader-follower relationships as directed edges, the overall traffic structure can be modeled as a directed graph, which we refer to as the leader-follower network.

The process then diverges into two branches. In Branch A (highlighted with diagonal shading in Fig. 3), candidate groups, i.e., subnetworks frequently appearing in the leader-follower network, are extracted for each time frame. The frequency of each candidate subnetwork i is quantified as λ_i^O , the average number of occurrences per unit time across the entire observation period.

Branch B (highlighted with a dotted background) introduces a randomized baseline. Here, the vehicle nodes of the observed leader-follower network are randomly shuffled, preserving vehicle-type labels (“m,” “r,” “c,” “h”) to retain type-specific characteristics. This process is repeated multiple times to construct randomized networks, from which the average occurrence frequency of subnetwork i , denoted as λ_i^U , is computed. In Fig. 3, λ_{ji}^S indicates the average occurrence of i in the j -th randomized network.

Using the observed λ_i^O and the randomized λ_i^U , we construct two Poisson distributions representing the expected number of occurrences per unit time for each subnetwork. If the distribution derived from λ_i^O is statistically higher than that from λ_i^U , subnetwork i is inferred to exhibit a significant tendency toward group formation and is thus classified as a *group*.

For example, according to a previous study [20], a pair of motorcycles maintaining a leader–follower relationship is considered a typical group in the AF. In such cases, as illustrated in Figure 4 (a), the leader–follower relationship between two motorcycles tends to be sustained over a long period and is frequently generated. The arrows in Figure 4 (a) represent leader–follower relationships. Even a momentary leader–follower interaction between two upstream motorcycles at time t_3 is identified as a group. Figure 4 (b) shows an actual snapshot in which two motorcycles with a leader–follower relationship are detected as a group in real traffic. In this example, although three motorcycles are arranged in a leader–follower sequence, the two motorcycles at the front and the two at the rear form separate groups based on their respective leader–follower relationships.

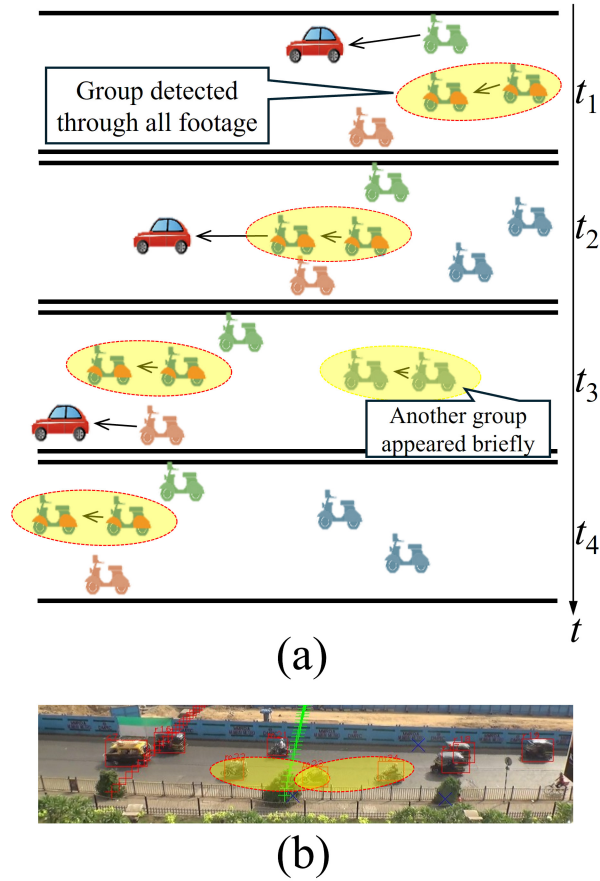


Fig. 4. (a) Conceptual image of a group in traffic: an example where two motorcycles maintaining a leader–follower relationship are detected as a group. (b) Actual traffic scene where a group of two motorcycles is detected.

2.4 Applied PCUs

Various methods for estimating PCU have been proposed, as reviewed by Sharma et al. [30]. In this study, we apply three PCU estimation methods with different theoretical backgrounds to enhance the robustness of the analysis and reduce dependence on any specific estimation method. Specifically, we use (1) the interpolation-based method described in the Indian Highway Capacity Manual [6] (hereinafter referred to as IP), (2) the multiple linear regression method (MLR) [30], and (3) the method based on the projected area and speed of each vehicle type (hereinafter referred to as Speed-based, SB) [7]. In this section, we provide an overview of each PCU estimation method.

IP method The IP method estimates the PCU value y (PCU) of a given vehicle type by interpolating from its proportion $x\%$ in the traffic flow.

The parameters used for interpolation are shown in Table 1 [6]. x_1 represents the lower bound of the expected proportion of each vehicle type in traffic, and x_2 represents the upper bound. Similarly, y_1 denotes the estimated PCU value when the proportion of a given vehicle type is $x_1\%$, and y_2 denotes the estimated PCU value when the proportion is $x_2\%$. In this study, the vehicle types {m, r, c, h} are treated as two-wheelers (TW), auto-rickshaws (Auto), small cars (SC), and trucks (TAT), respectively, as defined in Table 1.

Vehicle Type	y_1	y_2	x_1	x_2
Standard Car(SC)	1.0	1.0	6	30
Big Car(BC)	1.1	2.5	5	16
Motorized Two Wheeler(TW)	0.2	0.5	17	64
Auto rikishaw(Auto)	1.1	2.0	5	19
Bus(B)	2.8	4.8	5	10
Light Commercial Vehicle(LCV)	2.0	5.0	2	18
Two /Three Axle Truck(TAT)	3.0	5.5	5	20
Multi Axle Trucks / Vehicle(MAT)	4.6	14.6	2	11
Tractor Trailer(TT)	5.0	8.0	2	5

Table 1. Parameters utilized in the IP method [6]

Furthermore, the interpolation formula used to estimate the PCU value based on the proportion $x\%$ of each vehicle type in each video frame is shown in Equation 1.

$$y = y_1 + \left(\frac{y_2 - y_1}{x_2 - x_1} \right) \times (x - x_1) \quad (1)$$

where

y = the estimated PCU value of a certain vehicle type,

x = the proportion of a certain vehicle type in the traffic,

x_1 = lower boundary of proportion of a certain vehicle type,

x_2 = upper boundary of proportion of a certain vehicle type,

y_1 = lower boundary of PCU value of a certain vehicle type,

y_2 = upper boundary of PCU value of a certain vehicle type.

If the vehicle type proportion in a frame falls below the lower bound x_1 , the estimated PCU value for that frame is set to y_1 . Conversely, if the proportion exceeds the upper bound x_2 , the estimated PCU value is set to y_2 . Note that in the IP method, vehicle type proportions are calculated based on the number of vehicles (i.e., vehicle count-based).

MLR method In the MLR method [30], the regression coefficient a_j for each vehicle type is first obtained through multiple linear regression analysis using the average speed of passenger cars and the traffic flow of each vehicle type, as expressed in Equation 2.

$$V_c = a_0 + \sum_{j=m,r,c,h} a_j Q_j \quad (2)$$

where

V_c : average speed of passenger cars (km/h),

Q_j : = flow of vehicle type j (vehicle/h),

j : index representing vehicle types. $j = m, r, c, h$ for motorcycles, auto rickshaws, passenger cars, and heavy vehicles, respectively,

a_0 = intercept,

a_j = regression coefficients for vehicle type j ,

In general, as traffic flow increases, vehicle speed tends to decrease. The regression coefficient a_j represents the extent to which vehicle type j contributes to the reduction in the speed of passenger cars in traffic. This regression analysis determines a total of five parameters, including the intercept a_0 and the four coefficients a_j . Given the interpretation of these coefficients, each a_j is expected to be negative. Moreover, the larger the absolute value of a_j , the greater the impact that vehicle type j has on the speed of passenger cars and other vehicles in the traffic flow.

Finally, the PCU value for each vehicle type is calculated from the regression coefficients obtained through the regression analysis, using Equation 3.

$$PCU_j = \frac{a_j}{a_c} \quad (3)$$

Moreover, since the MLR method uses both traffic flow and speed, the regression coefficients may vary depending on the traffic situation. In this study, we divided the data into the four traffic situations defined in Section 2.2, and performed regression analysis separately for each situation to obtain the corresponding regression coefficients and PCU values. Calculated PCU values are listed in Table 2.

Note that the MLR-based PCU in this study is an operational equivalence factor defined as a ratio of marginal effects on passenger-car speed, rather than a measure of physical size or space occupancy. Therefore, depending on the traffic situation, the estimated PCU values may exceed one or deviate from intuitive size-based expectations. In addition, because coefficient-ratio-based estimates can be unstable, we also employ the IP and SB methods to reduce method dependence and to check the robustness of the findings.

Table 2. PCU values for respective vehicle types in respective traffic situations.

Traffic situation	c	m	r	h
AF	1.00	5.17	2.77	1.35
DJ	1.00	2.10	1.16	4.44
AJ	1.00	0.62	0.72	1.41
OT	1.00	0.16	1.32	0.63

SB method The SB method [30] estimates the PCU based on the projected area and speed of each vehicle type, using the calculation shown in Equation 4.

$$PCU_j = \frac{V_c/V_j}{A_c/A_j} \quad (4)$$

where

V_j, V_c = average speed of vehicle type j and passenger cars, respectively

A_j, A_c = projected area of vehicle type j and passenger cars on the road, respectively

The numerator in Equation 4 represents the ratio of the average speed of the target vehicle type to that of passenger cars, while the denominator represents the ratio of the projected area of the target vehicle type to that of passenger cars. To calculate the projected area, the length of each vehicle in the image coordinate system was converted to real-world coordinates using a homography matrix. The vehicle widths were uniformly set to 1.7 m for passenger cars, 2.5 m for heavy vehicles, 0.8 m for two-wheelers, and 1.3 m for auto-rickshaws, since the video was recorded from an oblique angle above the road, making it difficult to accurately measure vehicle widths. The projected area of a vehicle is calculated as the vehicle width multiplied by the length. For each frame, the projected area of each vehicle type was calculated by averaging the total projected area of all vehicles of that type in the frame, and this average was used as the representative projected area of that vehicle type.

In the subsequent sections, we calculate traffic density and flow based on the PCU values described above and construct fundamental diagrams. The proportion of groups in the traffic (either on a vehicle-count basis or a PCU-weighted basis) is calculated for each frame, and the data points are distinguished accordingly in the diagrams. This approach forms the basis for the analyses presented in Section 3 and beyond.

3 Effect of Group Proportion on the Flow-Density Structure

To investigate how the proportion of groups in traffic affects macroscopic traffic behavior, we analyze the relationship between flow and density under varying group proportions. Two definitions of group proportion are considered: the vehicle-count-based proportion, which reflects the number of vehicles, and the PCU-based proportion, which accounts for the PCU of each vehicle type. For example, let us assume that the PCU of a motorcycle is 0.5, while that of a car is 1.0. In the traffic situation depicted at the top of Figure 4(a), the PCU-based group proportion is 1.0/3.0 because the total PCU of all vehicles in the traffic is 3.0, and the group itself accounts for 1.0 PCU. Meanwhile, the vehicle-count-based group proportion is 2/5, as there are five vehicles in total, two of which belong

to the group. By comparing flow-density relationships across these proportions, we aim to reveal how the presence of groups influences traffic characteristics in terms of flow contribution.

This section presents two complementary visualizations. First, a smoothed analysis using segment-wise medians highlights general trends across group proportions. Then, a more detailed scatter plot visualization exposes local variations and distributional differences within each group proportion. Together, these analyses provide both a macroscopic overview and a microscopic perspective on how group composition affects traffic flow dynamics. Besides, we examine whether the degree of vehicle-type mixing within a group is related to the flow performance.

3.1 Overview of Flow-Density Structure via Segment-Wise Medians

Result Figure 5 shows the flow-density relationship for each group proportion in traffic, illustrated with various lines. The background gray dots represent all the data points. Flow and density are calculated based on the PCU values defined by IP method. For each density value, the flow value shown is the median of flow values within ± 0.15 (PCU/m). This computation is repeated by shifting the density window in increments of 0.05 (PCU/m). When the number of data points within a window used to compute the median is fewer than 10, the median is not calculated and the corresponding flow-density curve is not plotted. The various lines represent these median values, and the percentage shown in the legend denotes the proportion of group vehicles in the traffic flow. Figure 5(a) specifically focuses on groups whose occurrence frequency λ_i^O was at least 0.5 (/frame), while Figure 5(b) expands the range to include groups with lower occurrence frequency, down to 0.1 (/frame). Since λ_i^O is the threshold of the occurrence frequency used to detect groups, Figure 5(a) shows the flow-density characteristics of vehicle groups that appear relatively frequently and are statistically concluded to be likely to form leader-follower relationships. In contrast, Figure 5(b) illustrates the characteristics of vehicle groups that appear less frequently but are nevertheless concluded to be likely to form leader-follower relationships.

From Figure 5(a), we can observe the following characteristics, labeled from (1) to (3). Additionally, Figure 5(b) reveals the characteristic described in (4).

- (1) When the group proportion is particularly small, the highest median flow among all conditions is observed.
- (2) When the group proportion is particularly large, relatively high flow values are observed across all conditions.
- (3) In the medium density range, the flow decreases as the group proportion increases.
- (4) In the high-density range, relatively large flow values are observed when the group proportion is moderate (20–40% or 40–60%).

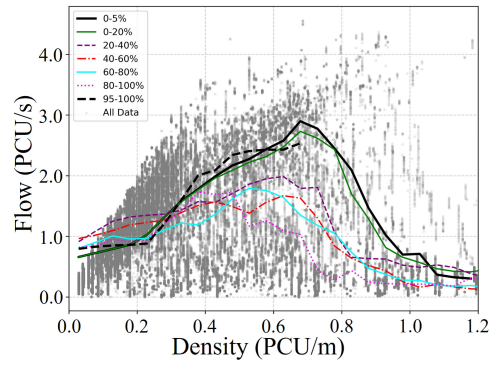
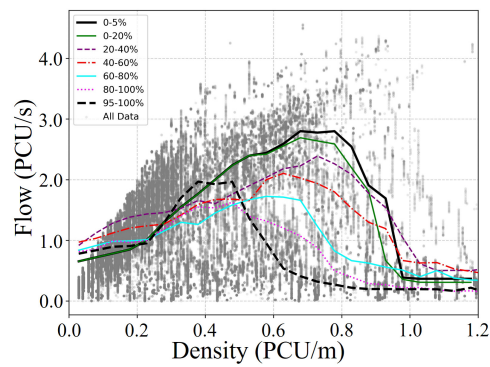
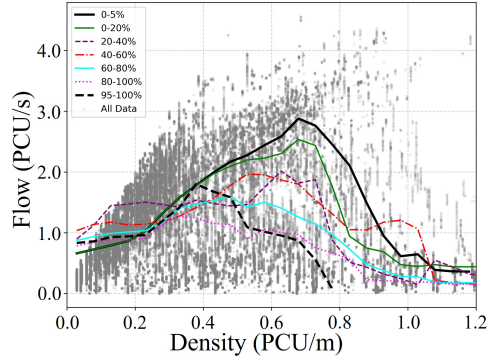
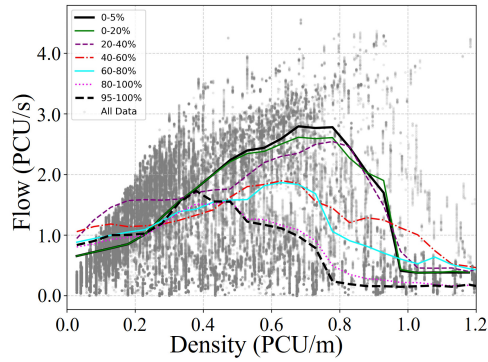
(a) Groups $\lambda_i^0 \geq 0.5$ (/frame) are considered.(b) Groups $\lambda_i^0 \geq 0.1$ (/frame) are considered.

Fig. 5. Medians of flow in PCU (IP method) for respective group proportion by number of vehicles. The percentage indicates the proportion of group vehicles in the traffic flow. λ_i^0 is the threshold of the occurrence frequency used to detect groups.

Figure 6 presents a counterpart to Figure 5 shown earlier, with group proportions computed based on PCU values.



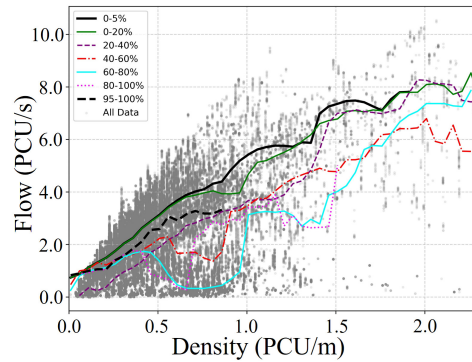
(a) Groups $\lambda_i^0 \geq 0.5$ (/frame) are considered.



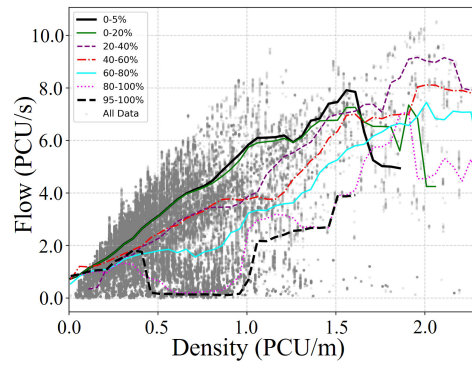
(b) Groups $\lambda_i^0 \geq 0.1$ (/frame) are considered.

Fig. 6. Medians of flow in PCU (IP method) for respective group proportion by PCU values.

Furthermore, Figures 7 and 8 show the flow-density relationships when PCU is calculated using the MLR method, and Figures 9 and 10 show those obtained using the SB method.

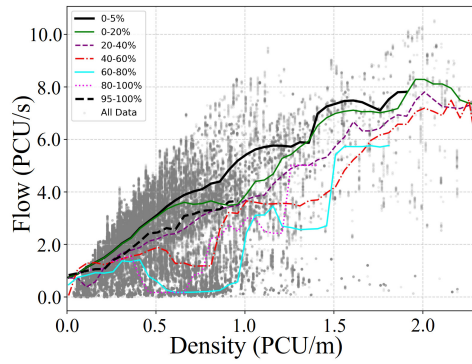


(a) Groups $\lambda_i^0 \geq 0.5$ (/frame) are considered.

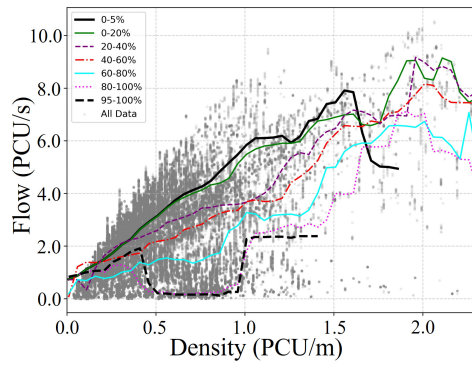


(b) Groups $\lambda_i^0 \geq 0.1$ (/frame) are considered.

Fig. 7. Medians of flow in PCU (MLR method) for respective group proportion by number of vehicles.

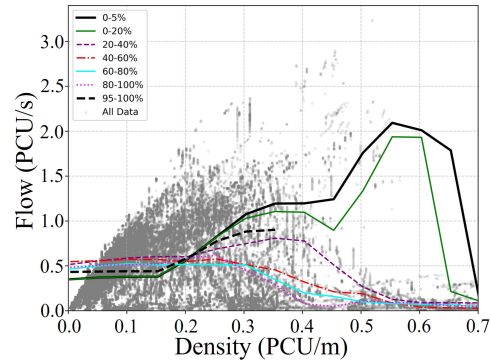


(a) Groups $\lambda_i^0 \geq 0.5$ (/frame) are considered.

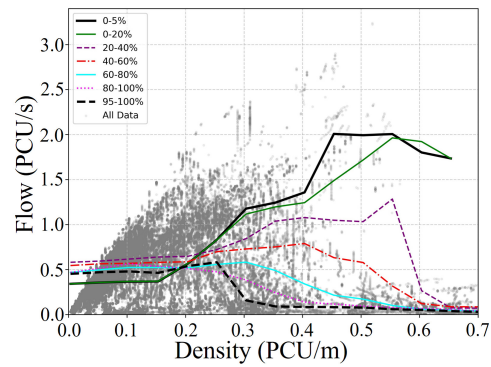


(b) Groups $\lambda_i^0 \geq 0.1$ (/frame) are considered.

Fig. 8. Medians of flow in PCU (MLR method) for respective group proportion by PCU values.

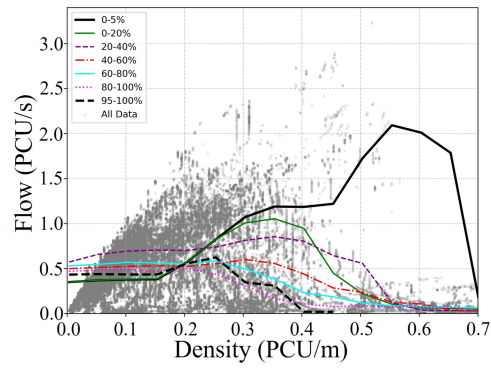


(a) Groups $\lambda_i^0 \geq 0.5$ (/frame) are considered.

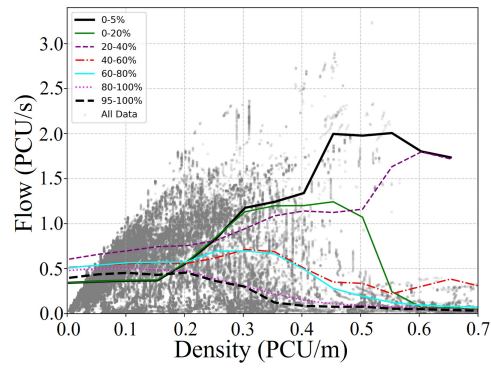


(b) Groups $\lambda_i^0 \geq 0.1$ (/frame) are considered.

Fig. 9. Medians of flow in PCU (SB method) for respective group proportion by number of vehicles.



(a) Groups $\lambda_i^0 \geq 0.5$ (/frame) are considered.



(b) Groups $\lambda_i^0 \geq 0.1$ (/frame) are considered.

Fig. 10. Medians of flow in PCU (SB method) for respective group proportion by PCU values.

The characteristics observed in Figures 5 through 10 are summarized in Tables 3 through 6. In the tables, the symbols indicate the level of support for each characteristic as follows: \bigcirc denotes that the characteristic is clearly supported by the data; \times indicates that the characteristic is not supported; Δ represents partial or ambiguous support, often due to limited data or variability. The superscripts provide additional notes on specific limitations or conditions under which the support is observed. The symbol $\bar{}$ indicates that the result is confirmed but with some limitations, while $^+$ indicates that the characteristic is generally unsupported, though minor exceptions may exist.

Table 3. Flow-density characteristics under vehicle-count-based group proportions ($\lambda_i^O \geq 0.5$ (/frame)).

Characteristic	IP	MLR	SB	Consensus
(1) When the group proportion is particularly small, the highest flow is observed among all conditions.	\bigcirc	Δ^a	\bigcirc	$\bar{\bigcirc}$
(2) When the group proportion is particularly large, relatively high flow values are observed.	\bigcirc	\times	\times	\times^+
(3) In the medium-density range, flow decreases as the group proportion increases.	$\bar{\bigcirc}^b$	Δ^c	$\bar{\bigcirc}^b$	$\bar{\bigcirc}$
(4) In the high-density range, relatively large flows are observed for moderate group proportions (20–40% or 40–60%).	\times	Δ^d	\times	\times^+

Notes:

- ^a No median data in very high density regions (> 1.8 PCU/m).
- ^b Excluding extremely large group proportions (95-100%).
- ^c The order is not strictly monotonic.
- ^d Based on limited data.
- ⁺ Majority vote, leaning toward support. $\bar{}$ Majority vote, leaning toward non-support.

Table 4. Flow-density characteristics under vehicle-count-based group proportions ($\lambda_i^0 \geq 0.1$ (/frame)).

Characteristic	IP	MLR	SB	Consensus
(1) When the group proportion is particularly small, the highest flow is observed among all conditions.	✗	✗	○	✗ ⁺
(2) When the group proportion is particularly large, relatively high flow values are observed.	✗	✗	✗	✗
(3) In the medium-density range, flow decreases as the group proportion increases.	○	○	○	○
(4) In the high-density range, relatively large flows are observed for moderate group proportions (20–40% or 40–60%).	△ ^d	△ ^d	△ ^e	△

Notes: Same as in Table 3.

^e Observed only in specific density intervals.

Table 5. Flow-density characteristics under PCU-based group proportions ($\lambda_i^0 \geq 0.5$ (/frame)).

Characteristic	IP	MLR	SB	Consensus
(1) When the group proportion is particularly small, the highest flow is observed among all conditions.	○	△ ^a	○	○ ⁻
(2) When the group proportion is particularly large, relatively high flow values are observed.	✗	✗	✗	✗
(3) In the medium-density range, flow decreases as the group proportion increases.	○	△ ^c	○	○ ⁻
(4) In the high-density range, relatively large flows are observed for moderate group proportions (20–40% or 40–60%).	△ ^e	△ ^d	△ ^e	△

Notes:

^a No median data in very high density regions (> 1.8 PCU/m).

^c The order is not strictly monotonic.

^d Based on limited data.

^e Observed only in specific density intervals.

⁺ Majority vote, leaning toward support. ⁻ Majority vote, leaning toward non-support.

Table 6. Flow-density characteristics under PCU-based group proportions ($\lambda_i^0 \geq 0.1$ (/frame)).

Characteristic	IP	MLR	SB	Consensus
(1) When the group proportion is particularly small, the highest flow is observed among all conditions.	✗	✗	○	✗ ⁺
(2) When the group proportion is particularly large, relatively high flow values are observed.	✗	✗	✗	✗
(3) In the medium-density range, flow decreases as the group proportion increases.	○	○	△ ^c	○ ⁻
(4) In the high-density range, relatively large flows are observed for moderate group proportions (20–40% or 40–60%).	△ ^d	△ ^d	✗	△ ⁻

Notes: Same as in Table 5.

Discussion Characteristic (1) is predominantly observed under conditions where frequently appearing groups are absent from traffic, i.e., groups with $\lambda_i^O \geq 0.5$ are not present. Instead, the maximum flow tends to be achieved in the presence of a certain proportion of less frequent groups with $0.1 \leq \lambda_i^O < 0.5$ (/frame).

As reported in [20], groups falling within the range $\lambda_i^O \geq 0.1$ are generally composed of larger vehicles and exhibit greater member counts compared to those in the $\lambda_i^O \geq 0.5$ range. Accordingly, Characteristic 1 can be interpreted as a reflection of traffic in which increased density facilitates the emergence of such less frequent, larger groups—resulting in enhanced flow—thereby constituting a plausible outcome. On the other hand, Characteristic (2) does not consistently hold across all conditions. Taken together with Characteristic (1), the findings suggest that an increase in group proportion alone does not guarantee a corresponding increase in traffic flow. Rather, the presence of moderately frequent groups, specifically those with $0.1 \leq \lambda_i^O < 0.5$ (/frame), appears to play a crucial role in enabling maximum flow conditions.

Characteristic (3) is observed robustly, irrespective of the method used to compute group proportion or the frequency of group occurrence. This robustness can be attributed to the formation of vehicle clusters generated by deceleration waves at moderate densities, which are likely being captured as groups in the analysis in [20].

Lastly, Characteristic (4) tends to manifest more clearly when group proportions are calculated based on PCU. The finding that moderate group proportions lead to relatively high flow in high-density regions is similar to the behavior observed in Characteristic (1). This suggests that adjusting group composition may be a viable strategy for improving traffic performance. Furthermore, the result underscores the importance of employing PCU-based group proportions when assessing their impact on macroscopic traffic characteristics.

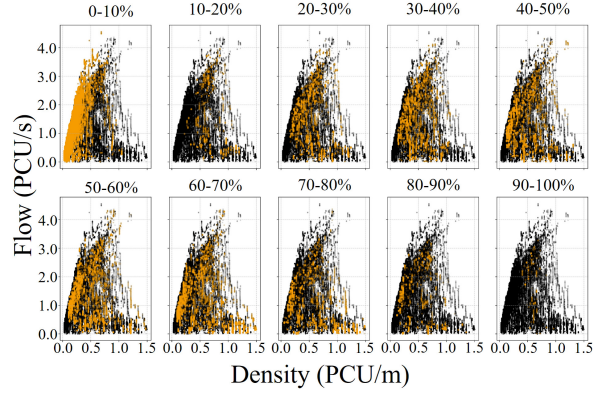
3.2 Detailed Visualization of Group-Wise Variability in Flow-Density Data

Result Figure 11 illustrates the flow-density relationships for different ranges of group proportions, shown as orange scatter plots. The group proportions are calculated based on the number of vehicles. The black background dots represent all available data points. Both flow and density are computed using PCUs derived from the IP method. Specifically, Figure 11(a) displays the flow-density relationships for groups with an occurrence frequency of $\lambda_i^O \geq 0.5$ (/frame), whereas Figure 11(b) covers groups with $\lambda_i^O \geq 0.1$ (/frame).

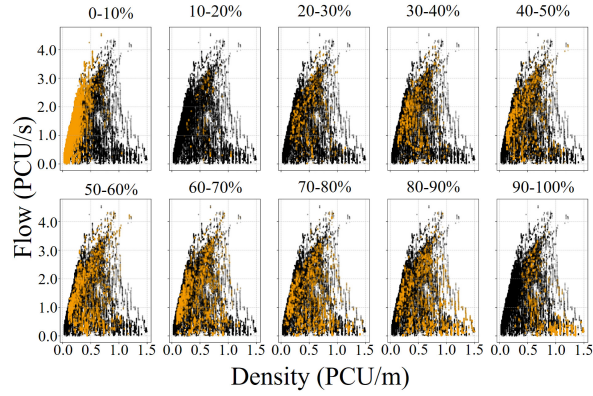
The following characteristics, labeled from (A) to (G), are identified from Figure 11:

- (A) When the group proportion is between 0–10%, the data are concentrated in the high-flow, free-flow regime.
- (B) When the group proportion is between 0–10%, high-density states are rarely observed.
- (C) In the 10–20% group proportion range, data points at low densities are reduced.
- (D) The highest flow values are achieved when the group proportion lies in the moderate range of 30–60%.
- (E) As the group proportion increases beyond 50%, the number of data points in the medium-density and medium-flow region decreases.

- (F) In the 90–100% group proportion range, high-density states do not occur.
 (G) In the 90–100% group proportion range, low-density states do not occur.



(a) Groups $\lambda_i^0 \geq 0.5$ (/frame) are considered.

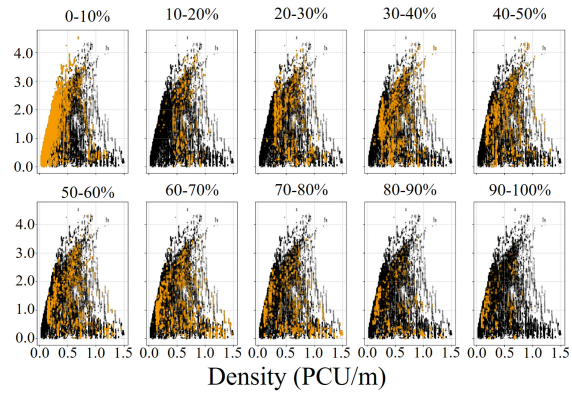


(b) Groups $\lambda_i^0 \geq 0.1$ (/frame) are considered.

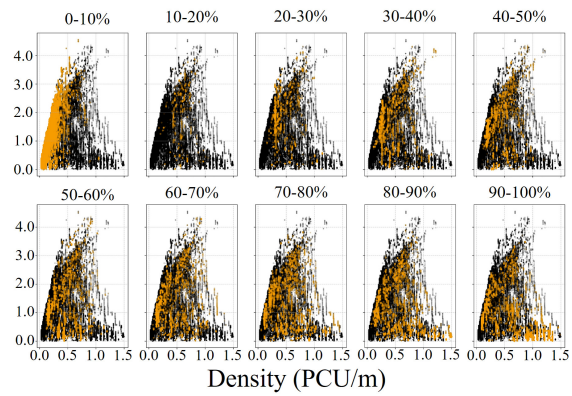
Fig. 11. Scatter plot of flow in PCU (IP method) for respective group proportion by number of vehicles.

Figure 12 presents the same group proportion analysis as shown in Figure 11, but with group proportions calculated based on PCU in IP method.

Furthermore, Figures 13 and 14 show the flow-density relationships based on PCU values computed using the MLR method, while Figures 15 and 16 present the corresponding relationships derived using the SB method, all illustrated as scatter plots.

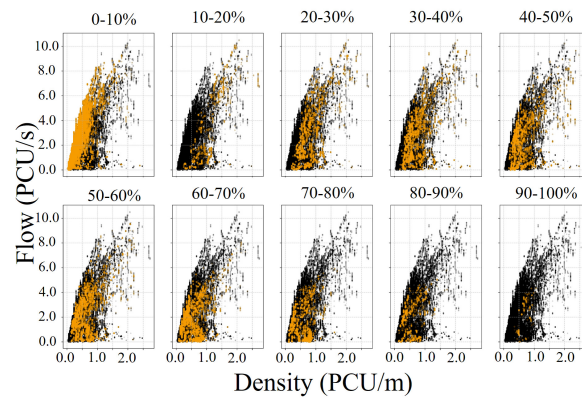


(a) Groups $\lambda_i^0 \geq 0.5$ (/frame) are considered.

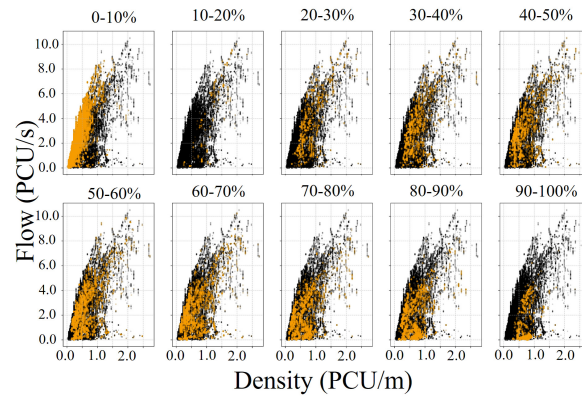


(b) Groups $\lambda_i^0 \geq 0.1$ (/frame) are considered.

Fig. 12. Scatter plot of flow in PCU (IP method) for respective group proportion by PCU.

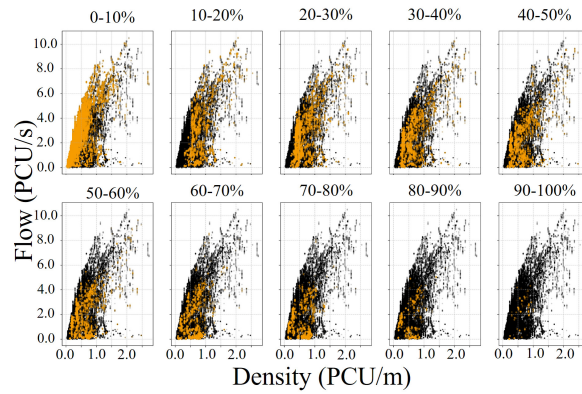


(a) Groups $\lambda_i^0 \geq 0.5$ (/frame) are considered.

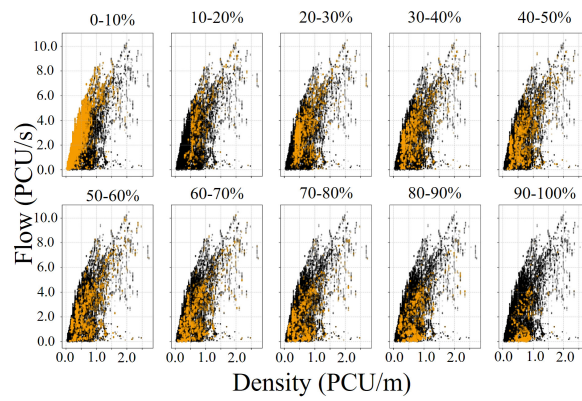


(b) Groups $\lambda_i^0 \geq 0.1$ (/frame) are considered.

Fig. 13. Scatter plot of flow in PCU (MLR method) for respective group proportion by number of vehicles.

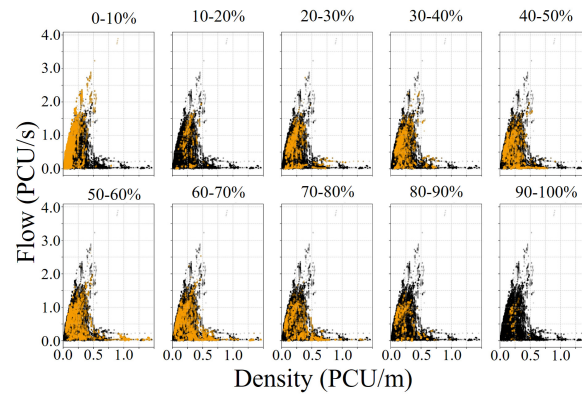


(a) Groups $\lambda_i^0 \geq 0.5$ (/frame) are considered.

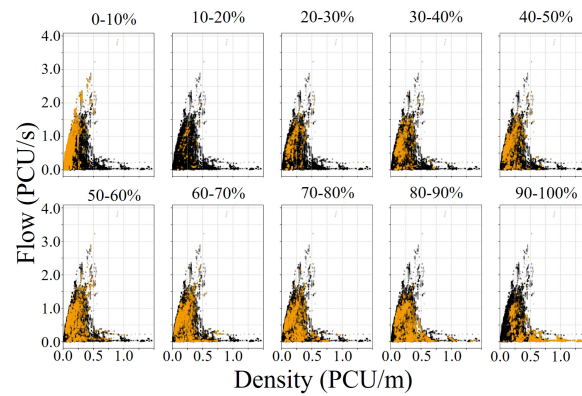


(b) Groups $\lambda_i^0 \geq 0.1$ (/frame) are considered.

Fig. 14. Scatter plot of flow in PCU (MLR method) for respective group proportion by PCU.

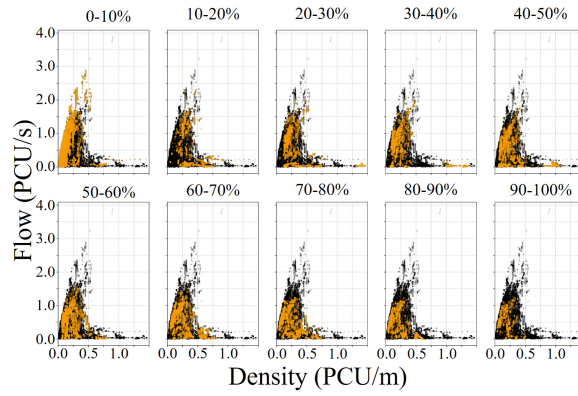


(a) Groups $\lambda_i^0 \geq 0.5$ (/frame) are considered.

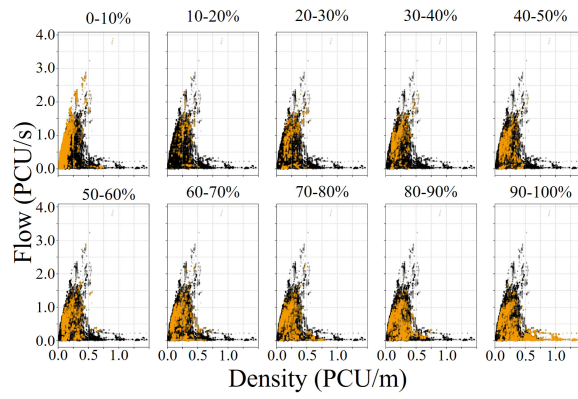


(b) Groups $\lambda_i^0 \geq 0.1$ (/frame) are considered.

Fig. 15. Scatter plot of flow in PCU (SB method) for respective group proportion by number of vehicles.



(a) Groups $\lambda_i^0 \geq 0.5$ (/frame) are considered.



(b) Groups $\lambda_i^0 \geq 0.1$ (/frame) are considered.

Fig. 16. Scatter plot of flow in PCU (SB method) for respective group proportion by PCU.

The characteristics observed in Figures 11 through 16 are summarized in Tables 7 through 10. In the tables, the symbols indicate the level of support for each characteristic as follows: \bigcirc denotes that the characteristic is clearly supported by the data; \times indicates that the characteristic is not supported; Δ represents partial or ambiguous support, often due to limited data or variability. In the ‘‘Consensus’’ column, we indicate whether each characteristic is universally supported (\bigcirc), partially supported (Δ), or considered unsupported (\times) by a majority vote based on the results of the three methods (IP, MLR, and SB). We adopt the symbol that appears most frequently among the three outcomes; if all three symbols are different, we assign Δ . In addition, when the three outcomes are $\{\bigcirc, \bigcirc, \times\}$ or $\{\bigcirc, \Delta, \bigcirc\}$, we denote the Consensus entry as \bigcirc^- to indicate that the characteristic is not fully supported. Conversely, when the three outcomes are $\{\bigcirc, \times, \times\}$ or $\{\times, \Delta, \times\}$, we denote the Consensus entry as \times^+ to indicate that the characteristic is not entirely unsupported.

Table 7. Flow-density characteristics under vehicle-count-based group proportions (scatter plot analysis) ($\lambda_i^0 \geq 0.5$ (frame)).

Characteristic	IP	MLR	SB	Consensus
(A) When the group proportion is 0–10%, data concentrate in the high-flow, free-flow regime.	\bigcirc	\bigcirc	\bigcirc	\bigcirc
(B) When the group proportion is 0–10%, high-density states are rarely observed.	\bigcirc	\bigcirc	\bigcirc	\bigcirc
(C) In the 10–20% group proportion range, low-density data points are scarce.	\bigcirc	\bigcirc	\bigcirc	\bigcirc
(D) The highest flow values are observed when the group proportion is in the moderate range of 30–60%.	\bigcirc	\bigcirc^f	\times	\bigcirc^-
(E) As the group proportion increases beyond 50%, medium-density and medium-flow data points decrease.	Δ	\bigcirc	Δ	Δ^+
(F) In the 90–100% group proportion range, high-density states do not occur.	\bigcirc	\bigcirc	\bigcirc	\bigcirc
(G) In the 90–100% group proportion range, low-density states do not occur.	\bigcirc	\bigcirc	\bigcirc	\bigcirc

Notes:

^f The highest flow values are also observed within the 10–20% group proportion range.

⁺ Majority vote, leaning toward support. ⁻ Majority vote, leaning toward non-support.

Table 8. Flow-density characteristics under vehicle-count-based group proportions (scatter plot analysis) ($\lambda_i^0 \geq 0.1$ (frame)).

Characteristic	IP	MLR	SB	Consensus
(A) When the group proportion is 0–10%, data concentrate in the high-flow, free-flow regime.	○	○	○	○
(B) When the group proportion is 0–10%, high-density states are rarely observed.	○	○	○	○
(C) In the 10–20% group proportion range, low-density data points are scarce.	○	○	○	○
(D) The highest flow values are observed when the group proportion is in the moderate range of 30–60%.	○	○ ^f	✗	○ ⁻
(E) As the group proportion increases beyond 50%, medium-density and medium-flow data points decrease.	△	△	✗	△ ⁻
(F) In the 90–100% group proportion range, high-density states do not occur.	✗	○	✗	✗ ⁺
(G) In the 90–100% group proportion range, low-density states do not occur.	○	○	○	○

Notes:

^f In some cases, the highest flow values are also observed within the 10–20% group proportion range.

⁺ Majority vote, leaning toward support. ⁻ Majority vote, leaning toward non-support.

Table 9. Flow-density characteristics under PCU-based group proportions (scatter plot analysis) ($\lambda_i^0 \geq 0.5$ (frame)).

Characteristic	IP	MLR	SB	Consensus
(A) When the group proportion is 0–10%, data concentrate in the high-flow, free-flow regime.	○	○	○	○
(B) When the group proportion is 0–10%, high-density states are rarely observed.	○	△	△	△ ⁺
(C) In the 10–20% group proportion range, low-density data points are scarce.	○	○	○	○
(D) The highest flow values are observed when the group proportion is in the moderate range of 30–60%.	○	○ ^g	✗	○ ⁻
(E) As the group proportion increases beyond 50%, medium-density and medium-flow data points decrease.	△	○	△	△ ⁺
(F) In the 90–100% group proportion range, high-density states do not occur.	○	○	○	○
(G) In the 90–100% group proportion range, low-density states do not occur.	✗	○	✗	✗ ⁺

Notes:

^g The highest flow values are also observed within the 0–20% group proportion range.

⁺ Majority vote, leaning toward support. ⁻ Majority vote, leaning toward non-support.

Table 10. Flow-density characteristics under PCU-based group proportions (scatter plot analysis) ($\lambda_i^0 \geq 0.1$ (/frame)).

Characteristic	IP	MLR	SB	Consensus
(A) When the group proportion is 0–10%, data concentrate in the high-flow, free-flow regime.	○	○	○	○
(B) When the group proportion is 0–10%, high-density states are rarely observed.	○	○	○	○
(C) In the 10–20% group proportion range, low-density data points are scarce.	○	○	○	○
(D) The highest flow values are observed when the group proportion is in the moderate range of 30–60%.	○	○ [‡]	✗	○ ⁻
(E) As the group proportion increases beyond 50%, medium-density and medium-flow data points decrease.	△	△	✗	△ ⁻
(F) In the 90–100% group proportion range, high-density states do not occur.	✗	○	✗	✗ ⁺
(G) In the 90–100% group proportion range, low-density states do not occur.	✗	○	✗	✗ ⁺

Notes:

[‡] The highest flow values are also observed within the 0–20% group proportion range.

⁺ Majority vote, leaning toward support. ⁻ Majority vote, leaning toward non-support.

Discussion Features (A) to (D) were consistently observed regardless of how group proportions were calculated or which threshold of λ_i^0 was used for group identification. Feature (A) suggests that in the free-flow regime, traffic flow increases when there is less velocity synchronization, indicating looser interactions among vehicles. Feature (B) shows that as density increases, velocity synchronization strengthens and group formation becomes more prominent, which is a natural result.

In contrast, Features (C) and (D) represent nontrivial phenomena. Two possible causal interpretations can be considered for Feature (C). First, “because the group proportion is outside the 10–20% range, low-density data points become scarce.” This implies that being in a group composition outside of 10–20% may contribute to increasing overall traffic density. Alternatively, considering the contraposition of the reverse causal direction, another interpretation is possible: “because the group proportion is in the 10–20% range, low-density data points still appear.” This suggests that only traffic composed of a moderate and relatively low group proportion can maintain a wide range of states, from low to high density, without changing the group composition. Furthermore, Feature (D) indicates an association between moderate group proportions (30–60%) and the highest flow rates. This finding complements Features 1 and 4 in Section 3.1, and together they suggest that adjusting group proportions could be a potential strategy for improving traffic flow.

Features (E) and (F) were observed only in cases where frequently appearing groups ($\lambda_i^0 \geq 0.5$ (/frame)) were used. Feature (F) indicates that large groups typically seen in high-density traffic do not appear frequently, which is a natural outcome. In contrast, Feature (E) reveals that when the group proportion exceeds 50%, the traffic tends to become extreme—either low- or high-density, or medium-density but with either very low or very high flow. While the exact cause of this remains unclear from the present analysis, one possible interpretation is that clusters formed by deceleration waves and detected as groups tend to result in low-speed and hence low-flow, medium-density traffic. Conversely, if the majority of group formation is due to autonomous coordination under other conditions than the deceleration waves, the traffic may be able to maintain high flow even at medium densities.

Finally, Feature (G) was observed only when the group proportion was computed on a vehicle-count basis. A vehicle-based group proportion of 90–100% effectively requires that almost all vehicles belong to some group; in particular, it requires that even small-PCU vehicles such as motorcycles simultaneously satisfy (i) stable leader–follower relations, (ii) speed synchronization, and (iii) sustained proximity. Such conditions are generally difficult to maintain in low-density traffic, where inter-vehicle distances are large, small vehicles can travel more freely, and platoon-like synchronization is less likely to persist. Therefore, it is natural that low-density states tend to be absent when the vehicle-count based group proportion reaches 90–100%. By contrast, a PCU-based group proportion can reach 90–100% even when some small vehicles remain outside groups (e.g., when groups are dominated by large-PCU vehicles), so the absence of low-density states is not necessarily expected. That said, if groups can be maintained even at low density—for example, by preserving larger headways while still moving cohesively—then low-density states could in principle occur even under vehicle-based 90–100% grouping.

3.3 Relationship between mean speed of groups and their entropy

Section 3.1 and Section 3.2 suggested that maintaining an appropriate group proportion may be associated with better traffic performance. In the final part of this section, we examine whether the degree of vehicle-type mixing within a group—quantified by entropy—is related to the mean speed achieved by that group, which serves as a proxy for flow performance. This analysis is intended to clarify whether entropy alone provides explanatory power for speed differences and, if so, what types of group structures might be desirable for enhancing traffic performance.

Note that, to quantify the degree of vehicle-type mixing within each group, entropy was used. On the one hand, the entropy is zero when a group consists of only one vehicle type. On the other hand, the entropy reaches one when a group contains an equal number of vehicles from each of the four vehicle types. The entropy is calculated using Equation 5:

$$\text{Entropy}_i = - \sum_{j=1}^4 p_{ij} \log_4 p_{ij} \quad (5)$$

where

j : Vehicle type j

p_{ij} : Occupation rate of type j in group i , based on the number of vehicle type j .

By using the logarithmic base of four, which corresponds to the number of vehicle types, the maximum value of entropy is normalized to 1. In calculating the group entropy, the value of p_{ij} is defined based on the number of vehicles of type j . This means, for example, that a group consisting of one motorcycle and one heavy vehicle is considered to have the same level of mixing as a group consisting of one motorcycle and one auto-rickshaw. Although it is also possible to consider mixing based on PCU, this study focuses on how vehicle types themselves are mixed. Therefore, the degree of mixing is measured using the number of vehicles.

Result For each traffic situation, we estimated an OLS regression of speed on entropy using all observations, and computed cluster-robust inference by clustering standard errors by group ID (i.e., an identifier for each unique combination of vehicle-type composition and leader–follower network structure). Table 11 reports the estimated slope for entropy, the 95% confidence interval based on cluster-robust standard errors, and the corresponding p-value, together with the number of observations (n_{points}) and clusters (n_{cluster}).

Under $\lambda_i^0 \geq 0.5$, the 95% confidence intervals of the entropy slopes include zero for all traffic states, and none of the slopes are statistically significant. Under $\lambda_i^0 \geq 0.1$, DJ shows a negative slope with a 95% confidence interval that does not include zero ($p = 0.027$), whereas the confidence intervals for AJ, OT, and AF include zero.

Discussion Table 11 shows that the estimated relationship between group entropy and speed is not robust across traffic situations or across the two frequency thresholds.

Under $\lambda_i^0 \geq 0.5$ (/frame), the 95% confidence intervals include zero for all traffic situations, indicating no statistically reliable association between entropy and speed at this threshold.

Table 11. All-observation regressions of speed on entropy with cluster-robust inference (clustered by group ID).

State	$\lambda_i^O \geq 0.5$ (/frame)					$\lambda_i^O \geq 0.1$ (/frame)				
	n_{points}	n_{cluster}	Slope	95% CI	p	n_{points}	n_{cluster}	Slope	95% CI	p
AJ	438,691	31	-0.205	[-0.51, 0.10]	0.184	438,691	31	0.396	[-0.16, 0.95]	0.153
OT	129,130	17	-0.585	[-1.39, 0.22]	0.145	129,130	17	-0.229	[-0.85, 0.39]	0.446
AF	209,109	4	-0.147	[-4.67, 4.38]	0.924	209,109	4	-1.373	[-3.63, 0.89]	0.149
DJ	301,155	10	0.360	[-0.29, 1.01]	0.240	301,155	10	-0.355	[-0.66, -0.05]	0.027

Under $\lambda_i^O \geq 0.1$ (/frame), DJ exhibits a negative slope whose 95% confidence interval does not include zero ($p = 0.027$), whereas AJ, OT, and AF remain non-significant with confidence intervals that include zero. However, this apparent DJ association does not replicate under $\lambda_i^O \geq 0.5$ (/frame), where the estimated slope becomes positive and non-significant.

Moreover, the slope sign is not stable across thresholds in some traffic situations (e.g., AJ and DJ), further suggesting that entropy alone does not provide a consistent explanation for speed variations.

Taken together, the state-wise analyses based on all observations with cluster-robust inference indicate that any association between entropy and speed, if present, is not consistent across traffic situations or across frequency thresholds.

4 Discussion through the all results

Tables 12–15 summarize only the consensus (majority-vote) results obtained from the segment-wise median analysis and scatter analysis. While the median analysis captures the representative trends of the flow–density structure, the scatter analysis complements it by preserving distributional constraints and extreme cases. By focusing on the consensus results, it becomes possible to distinguish features that are robust across both analyses from those that emerge depending on the aggregation method.

Table 12. Majority-vote summary of flow–density characteristics (segment-wise medians): vehicle-count-based group proportion.

Characteristic	$\lambda_i^O \geq 0.5$	$\lambda_i^O \geq 0.1$
(1) Particularly small group proportion yields the highest median flow.	○ ⁻	✕ ⁺
(2) Particularly large group proportion yields relatively high median flow.	✕ ⁺	✕
(3) In medium density, median flow decreases as group proportion increases.	○ ⁻	○
(4) In high density, moderate group proportions (20–40% or 40–60%) yield relatively large median flow.	✕ ⁺	△

Legend: ○ supported; △ partially/ambiguously supported; ✕ unsupported. ⁻: majority vote leans toward support but not fully consistent; ⁺: majority vote leans toward non-support but not entirely absent.

Table 13. Majority-vote summary of flow–density characteristics (segment-wise medians): PCU-based group proportion.

Characteristic	$\lambda_i^O \geq 0.5$	$\lambda_i^O \geq 0.1$
(1) Particularly small group proportion yields the highest median flow.	○ ⁻	✕ ⁺
(2) Particularly large group proportion yields relatively high median flow.	✕	✕
(3) In medium density, median flow decreases as group proportion increases.	○ ⁻	○ ⁻
(4) In high density, moderate group proportions (20–40% or 40–60%) yield relatively large median flow.	△	△ ⁻

Legend: Same as Table 12.

Table 14. Majority-vote summary of flow–density characteristics (scatter plots): vehicle-count-based group proportion.

Characteristic	$\lambda_i^O \geq 0.5$	$\lambda_i^O \geq 0.1$
(A) 0–10% group proportion concentrates in high-flow free-flow regime.	○	○
(B) 0–10% group proportion rarely exhibits high density.	○	○
(C) 10–20% group proportion has scarce low-density points.	○	○
(D) Highest flow is observed at moderate group proportion (30–60%).	○ ⁻	○ ⁻
(E) Beyond 50%, medium-density/medium-flow points decrease.	△ ⁺	△ ⁻
(F) At 90–100%, high density does not occur.	○	✕ ⁺
(G) At 90–100%, low density does not occur.	○	○

Legend: Same as Table 12.

Relatively robust features independent of proportion definitions and thresholds The majority-vote results based on the median analysis indicate that, in the intermediate-density regime, the relationship in which the median flow decreases as the group proportion increases (feature (3)) is generally supported regardless of the definition of the group proportion (vehicle-based or PCU-based) or the group extraction threshold λ_i^O (Tables 12 and 13). This suggests that, in the intermediate-density regime, an increase in the number of detected groups is typically accompanied by a reduction in speed, which in turn leads to a decrease in flow in the median sense. When vehicle clusters formed by deceleration are detected as groups, it is natural to interpret the resulting decrease in flow as a consequence of the associated speed reduction.

In contrast, the majority-vote results based on the scatter analysis indicate that the density regimes that are likely to be realized are constrained depending on the group proportion. In particular, the distributional features observed in the 0–10% and 10–20% proportion ranges (Features (A)–(C)) have been consistently observed across many settings, as described in detail in Section 3.2 (Tables 14–15). These results suggest that

Table 15. Majority-vote summary of flow–density characteristics (scatter plots): PCU-based group proportion.

Characteristic	$\lambda_i^0 \geq 0.5$	$\lambda_i^0 \geq 0.1$
(A) 0–10% group proportion concentrates in high-flow free-flow regime.	○	○
(B) 0–10% group proportion rarely exhibits high density.	△ ⁺	○
(C) 10–20% group proportion has scarce low-density points.	○	○
(D) Highest flow is observed at moderate group proportion (30–60%).	○ ⁻	○ ⁻
(E) Beyond 50%, medium-density/medium-flow points decrease.	△ ⁺	△ ⁻
(F) At 90–100%, high density does not occur.	○	✕ ⁺
(G) At 90–100%, low density does not occur.	✕ ⁺	✕ ⁺

Legend: Same as Table 12.

the group proportion may influence not only the magnitude of flow, but also the range of density that is observed, that is, whether low-density or high-density states are likely to appear. While it is certainly possible that

- the density state determines the group proportion through speed synchronization or cluster formation, it is also conceivable that
- the group proportion alters the reachable range of density states, or that
- a third factor, such as vehicle composition,

simultaneously affects both.

Where median and scatter diverge: differences between typical structures and extreme (high-flow) cases The most important difference appears in terms of which group proportion is associated with the maximum flow. In the scatter analysis, the tendency for the maximum flow to be observed at moderate group proportions (30–60%) (feature ((D))) is consistently supported as ○⁻. This suggests that high-flow points representing peak performance, which are relatively rare, tend to emerge at intermediate group proportions.

However, in the median-based results, the tendency for moderate group proportions to exhibit relatively large median flow in the high-density regime (feature (4)) receives at most partial support. Moreover, the claim that very large group proportions lead to high flow (Feature 2) is not supported under many conditions. Taken together, these findings indicate that the extreme high-flow cases captured by the scatter analysis and the typical flow–density structure captured by the median analysis do not necessarily coincide.

This suggests that, even under the same density and group proportion conditions, traffic can exhibit two distinct modes of behavior: a frequently observed low-efficiency state and a rare but high-efficiency state. More specifically, in the intermediate-density regime, an increase in groups caused by deceleration tends to be dominant, typically resulting in a reduction in flow. In contrast, at moderate group proportions, high-flow states may be observed as isolated points only when more cooperative configurations and motions are realized.

Sensitivity to the occurrence-frequency threshold λ_i^O From the consensus results, the distributional endpoint features observed in the scatter analysis in extreme group proportion ranges (90–100%)—such as the absence of realized high-density or low-density states—tend to depend on the choice of the occurrence-frequency threshold λ_i^O . For example, the result that high-density states are not realized in the 90–100% range (feature ((F))) is supported when only frequent groups are considered ($\lambda_i^O \geq 0.5$), whereas this tendency becomes weaker or is not supported when the threshold is relaxed to $\lambda_i^O \geq 0.1$ (Tables 14 and 15).

This suggests that, in extreme group proportion ranges, the endpoint features observed in the flow–density relationship are emphasized not so much by the group proportion itself as by the frequency of the groups that are extracted. One possible explanation is that, under extreme density conditions (either extremely low or extremely high densities), mechanisms may operate that make frequent groups less likely to be observed. At the low-density end, interactions between vehicles are weak and isolated driving becomes more prevalent, making it difficult for “groups” to form. In contrast, at the high-density end, large vehicle clusters are more likely to form, and as a result, small and frequent groups such as two-vehicle pairs may become relatively less observable. Consequently, when the analysis is restricted to frequent groups, the endpoints of the flow–density relationship are not sufficiently filled, and endpoint-like gaps tend to appear emphasized.

Conversely, although non-frequent groups are rare overall, they may tend to appear preferentially in extreme states (either near the high-density or low-density ends). When the threshold is relaxed, for example to $\lambda_i^O \geq 0.1$, such groups can fill the endpoints of the distribution, thereby weakening or rendering less visible the endpoint-like features.

Connection with entropy: entropy alone is insufficient and richer descriptors may be needed The entropy analysis (Section 3.3) indicates that the entropy–speed relationship is not robust across traffic situations. In particular, the state-wise estimates based on all observations with cluster-robust inference show that most effects are not statistically distinguishable from zero, and the sign is not stable across the two occurrence-frequency thresholds (Table 11). Although DJ under $\lambda_i^O \geq 0.1$ (/frame) shows a negative association, this pattern does not replicate under the stricter threshold.

Taken together, these results suggest that the internal composition of groups, as summarized by entropy alone, does not provide a robust explanation for speed variations across traffic situations. This does not rule out the possibility that internal structure matters; rather, it indicates that any effect is likely to depend on additional factors beyond entropy, such as the specific vehicle-type composition, interaction patterns, or traffic situation. Accordingly, linking group composition to traffic performance may require measures that describe group structure in greater detail, rather than relying on a single index such as entropy.

5 Conclusion

In heterogeneous disordered traffic, various types of vehicles interact without strict lane discipline, forming self-organized groups that may influence overall traffic performance.

While previous studies have shown evidence of such group formation, the impact of these groups on macroscopic traffic characteristics has remained unclear. This study aimed to clarify whether and how the prevalence and composition of vehicle groups affect flow–density relationships in heterogeneous disordered traffic.

By employing three different PCU estimation methods, we constructed flow–density diagrams that account for traffic heterogeneity and examined how varying group proportions affect traffic flow. To enhance the robustness of the analysis, we selected these PCU methods from different theoretical backgrounds. Besides, to strengthen the interpretability and robustness of the findings, we combined segment-wise median analysis and scatter analysis, which provide complementary views—the former capturing representative (typical) flow–density structures and the latter preserving distributional constraints and extreme cases—and then extracted robust tendencies via a consensus (majority-vote) comparison across settings.

Through the analysis, this study demonstrated that differences in group proportions exert complex effects on traffic flow depending on the traffic situation. It also showed that moderate group proportions can contribute to improved traffic performance under specific conditions. In addition, by contrasting the typical structures captured by medians with the extreme high-flow cases preserved in scatter plots, we highlighted that these two perspectives do not necessarily coincide, suggesting that traffic may exhibit qualitatively different modes even under similar density and proportion conditions. The main findings are summarized as follows.

First, group proportions were found to exert a nonlinear and traffic-situation-dependent effect on flow–density relationships. In particular, moderate group proportions (30–60%) consistently resulted in higher flow rates under medium- and high-density conditions. In contrast, when the group proportion exceeded 50%, the distribution of traffic tended to shift toward either low- or high-density extremes, with fewer observations in moderate-density ranges. Notably, the scatter analysis suggests that peak-performance (high-flow) cases tend to appear at moderate group proportions, whereas the median analysis indicates that, in intermediate-density regimes, increasing group proportion is typically associated with reduced representative flow; taken together, these results suggest the co-existence of a frequently observed lower-efficiency mode and a rarer but higher-efficiency mode.

Second, comparisons between group proportions based on vehicle counts and those based on PCUs revealed notable differences, especially when groups were composed predominantly of small-PCU vehicles such as motorcycles. This emphasizes the importance of selecting an appropriate normalization method when analyzing group effects in heterogeneous traffic environments to improve the flow.

Third, in free-flow conditions, lower group proportions tended to be associated with higher flow, suggesting that minimal inter-vehicle coordination can be advantageous when traffic is sparse. In contrast, under more congested conditions, moderate group proportions were more conducive to maintaining high flow levels.

Fourth, the entropy-based analysis of group composition did not show a consistent association between entropy and speed across traffic situations when using all observations with cluster-robust inference. Although DJ under $\lambda_i^0 \geq 0.1$ (/frame) showed a

negative association, this pattern did not replicate under the stricter threshold, suggesting that entropy alone is insufficient to robustly explain speed variations.

Finally, the contrast between the median and scatter analyses reveals that the representative flow–density structure and the extreme high-flow cases reflect different aspects of traffic behavior. While the median analysis captures the typical tendency that increasing group proportion in intermediate-density regimes is associated with reduced flow, the scatter analysis preserves rare but important high-flow points that emerge predominantly at moderate group proportions. This discrepancy indicates that, even under comparable density and group proportion conditions, traffic can alternate between a frequently realized, lower-efficiency state dominated by deceleration-induced clustering, and a less frequent but higher-efficiency state in which more cooperative configurations or collective motions are realized.

Overall, the findings demonstrate that the prevalence of self-organized groups and their proportion are closely related to macroscopic traffic dynamics in heterogeneous disordered traffic. At the same time, effects of internal composition captured by entropy were not robust across traffic situations, indicating that composition-related influences may require richer structural descriptors beyond a single entropy measure. These insights provide a foundation for designing group-aware traffic control strategies aimed at enabling bottom-up flow improvement, particularly in environments with limited infrastructure or formal regulation.

Acknowledgement

We thank Naotaka Ishizawa, Prashant Walawalkar, and other members of NYK Auto Logistics (India) Private Ltd. for their support with field observations in India. We express our gratitude to Akihiro Fujita for his help with field observations in India. We also thank Chuuya Osugi, Ryo Kondo, Zhiyan Xie, Satoshi Yamamoto, Chenkai Zhang, Munkhtushig Munguntsetseg, and Ryo Kawazu for their invaluable support in analyzing the video footage.

Funding

This study was supported in part by a research grant for Exploratory Research on Sustainable Humanosphere Science from the Research Institute for Sustainable Humanosphere (RISH) Kyoto University. This work was also supported by JSPS KAKENHI grant numbers 25287026, 18H05923, 19K15246, and 23K13512 and partially supported by MEXT under “Priority Issues and Exploratory Challenges on post-K (Supercomputer Fugaku)” (Exploratory Challenge 2: Construction of Models for Interaction Among Multiple Socioeconomic Phenomena, Model Development, and its Applications for Enabling Robust and Optimized Social Transportation Systems) (Project ID: hp190163).

Declaration of generative AI and AI-assisted technologies in the manuscript preparation process

During the preparation of this work the authors used ChatGPT in order to translate part of the text from Japanese and/or for grammar check/proof-reading. After using this tool/service, the authors reviewed and edited the content as needed and take full responsibility for the content of the published article.

References

1. Aghabayk, K., Young, W., Sarvi, M., Wang, Y.: Examining vehicle interactions during a vehicle-following manoeuvre. In: Australasian Transport Research Forum (ATRF), 34th, 2011, Adelaide, South Australia, Australia, vol. 34 (2011)
2. Akbar, P.A., Couture, V., Duranton, G., Storeygard, A.: The fast, the slow, and the congested: Urban transportation in rich and poor countries. Tech. rep., National Bureau of Economic Research (2023)
3. Babenko, B., Yang, M.H., Belongie, S.: Visual tracking with online multiple instance learning. In: 2009 IEEE Conference on computer vision and Pattern Recognition, pp. 983–990. IEEE (2009)
4. Bhardwaj, A., Iyer, S.R., Ramesh, S., White, J., Subramanian, L.: Understanding sudden traffic jams: From emergence to impact. *Development Engineering* **8**, 100105 (2023)
5. Calatayud, A., Sánchez González, S., Bedoya-Maya, F., Giraldez Zúñiga, F., Márquez, J.M.: Urban road congestion in latin america and the caribbean: Characteristics, costs, and mitigation (2021). DOI 10.18235/0003149. URL <https://doi.org/10.18235/0003149>
6. Chandra, S., Gangopadhyay, S., Velmurugan, S., Ravinder, K.: Indian highway capacity manual (indo-hcm) (2017)
7. Chandra, S., Kumar, Sikdar, P.K.: Dynamic pcu and estimation of capacity of urban roads. *Indian highways* **23** (1995). URL <https://api.semanticscholar.org/CorpusID:110038427>
8. Chen, D., Ahn, S., Bang, S., Noyce, D.: Car-Following and Lane-Changing Behavior Involving Heavy Vehicles. *Transportation Research Record: Journal of the Transportation Research Board* (2561), 89–97 (2016)
9. Chen, D., Li, J., Zhang, H.M.: Evidence and quantification of cooperation of driving agents in mixed traffic flow (2025). URL <https://arxiv.org/abs/2408.07297>
10. Das, S., Maurya, A.K., Rathi, S.: Modelling lateral movement behaviour of motorcycles in non-lane-based heterogeneous traffic using cellular automata. *Transportmetrica B: Transport Dynamics* **5**(2), 213–236 (2017)
11. Elmansouri, O., Almhroog, A., Badi, I.: Urban transportation in libya: An overview. *Transportation research interdisciplinary perspectives* **8**, 100161 (2020)
12. Fattah, M.A., Morshed, S.R., Kafy, A.A.: Insights into the socio-economic impacts of traffic congestion in the port and industrial areas of chittagong city, bangladesh. *Transportation Engineering* **9**, 100122 (2022)
13. King, M.: Traffic behaviour and compliance with the law in low and middle income countries: are we observing 'pragmatic driving'? In: *Proceedings of the 2015 Australasian Road Safety Conference (ARSC2015)*, pp. 1–11. Australasian College of Road Safety (ACRS) (2015)
14. Kumar, S., Mitra, S.: Self-organizing traffic at a malfunctioning intersection. *Journal of Artificial Societies and Social Simulation* **9**(4) (2006)
15. Lee, J., Park, B., Smith, B.L.: Agent-based modeling of motorcycle behavior at signalized intersections. *Transportation Research Record* **2560**, 101–109 (2016)

16. Lee, T.C.: An agent-based model to simulate motorcycle behaviour in mixed traffic flow. Ph.D. thesis, Imperial College London (University of London) (2007)
17. Li, J., Chen, D., Zhang, M.: Equilibrium modeling of mixed autonomy traffic flow based on game theory. *Transportation research part B: methodological* **166**, 110–127 (2022)
18. Liu, L., Zhu, L., Yang, D.: Modeling and simulation of the car-truck heterogeneous traffic flow based on a nonlinear car-following model. *Applied Mathematics and Computation* **273**, 706–717 (2016)
19. Mason, A.D., Woods, A.W.: Car-following model of multispecies systems of road traffic. *Physical Review E* **55**(3), 2203 (1997)
20. Nagahama, A., Nishinari, K.: Grouping mechanisms of vehicles in heterogeneous traffic with weak lane discipline: A single-site observational study focusing on leader–follower relations. *Physica A: Statistical Mechanics and its Applications* p. 131032 (2025)
21. Nagahama, A., Wada, T.: Response time and deceleration affected by lateral shift of leaders in vehicular traffic with weak lane discipline. In: *Traffic and Granular Flow 2019*, pp. 539–546. Springer (2020)
22. Nagahama, A., Wada, T., Takadama, K., Yanagisawa, D., Nishinari, K., Tanaka, K.: Prototype models for predicting vehicle types generated in heterogeneous traffic simulation. In: *International Conference on Traffic and Granular Flow*, pp. 431–438. Springer (2022)
23. Nagahama, A., Wada, T., Yanagisawa, D., Nishinari, K.: Detection of leader-follower combinations frequently observed in mixed traffic with weak lane-discipline. *Physica A: Statistical Mechanics and its Applications* **570**, 125789 (2021). DOI 10.1016/j.physa.2021.125789
24. Nagahama, A., Wada, T., Yanagisawa, D., Nishinari, K.: Certain types of vehicles in heterogeneous traffic in india tend to gather. *Journal of the Eastern Asia Society for Transportation Studies* **14**, 1794–1813 (2022)
25. Nagahama, A., Yanagisawa, D., Nishinari, K.: Dependence of driving characteristics upon follower–leader combination. *Physica A: Statistical Mechanics and its Applications* **483**, 503–516 (2017)
26. Phogat, A., Gupta, R., Kumar, E.N.: Study on effect of mixed traffic in highways. *International Research Journal of Engineering and Technology (IRJET)* **7**(01) (2020)
27. Samal, S.R., Mohanty, M., Santhakumar, S.M.: Adverse effect of congestion on economy, health and environment under mixed traffic scenario. *Transportation in Developing Economies* **7**(2), 15 (2021)
28. Sarvi, M.: Heavy commercial vehicles-following behavior and interactions with different vehicle classes. *Journal of advanced transportation* **47**(6), 572–580 (2013)
29. Sayer, J.R.: The effect of lead-vehicle size on driver following behavior (2000)
30. Sharma, A., Mathew, T.K.: Estimation of passenger car units for heterogeneous traffic using a microscopic simulation model. *Journal of Traffic and Transportation Engineering (English Edition)* **8**(5), 715–727 (2021)
31. Shiomi, Y., Nishiuchi, H.: Evaluation of spatial motorcycle segregation at isolated signalized intersections considering traffic flow conditions. *Journal of the Eastern Asia Society for Transportation Studies* **9**, 1644–1659 (2011)